Support provision to SAF development of the fractional snow cover product SCA and its independent validation

H-SAF Associated Scientist Program (HSAF_CDOP2_VS14_02)

Final report

14 October 2015

Kristin Böttcher[(1)], Sari Metsämäki[(1)], Panu Lahtinen[(2)]

(1) Finnish Environment Institute (SYKE), Helsinki, Finland
(2) Finnish Meteorological Institute (FMI), Helsinki, Finland

Table of Contents

Acronyms

AVHRR	Advanced Very High Resolution Radiometer
H12	Hydrosaf SCA product (featuring Snow Cover Fraction), formerly HSAF SN-obs3
MODIS	Moderate Resolution Imaging Spectroradiometer
NDSI	Normalized Difference Snow Index
NDVI	Normalized Difference Vegetation Index
SCA	Snow Covered Area
RMSD	Root Mean Square Deviation
SYKE	Finnish Environment Institute
VS	Visiting Scientist

1 Introduction

This document describes the results of the study "Support provision to SAF development of the fractional snow cover product (SCA) and its independent validation" carried out within the framework of the EUMETSAT SAF in support to Hydrology (H-SAF) at the Finnish Environment Institute.
For the retrieval of SCA, based on the *SCAmod* algorithm by Metsämäki et al. (2005), auxiliary information of the transmissivity of the forest is needed. The currently employed transmissivity map, originally provided for H-SAF SN-obs3 (presently H12) production by the Finnish Environment Institute (SYKE), has been used for 5 years. Recent development work at SYKE, where the applied algorithm was originally developed, provided an improved methodology for the estimation of transmissivity based on statistical relationship of land cover classification and at-satellite observed reflectances over the target area. Also other developments for the SCA retrieval procedure have been made at SYKE during last few years; the inclusion of those advances was also a topic of the VS-work. It was expected that the H-SAF H12 Fractional Snow Cover product would benefit from the update with an improved methodology.

Codice campo modificato

The objectives of this study were therefore:

(1) To study the possibility to improve the SCAmod-based SCA retrievals of H-SAF by updating the transmissivity map and by adapting two additional features into SCA-calculations.

(2) To compare the SCA-product by applying the new transmissivity input against current operational H-SAF SCA products.

(3) To validate the new improved H12 SCA against high resolution satellite images.

Chapter 2.22 provides the description of the methodology and results for the improvement of the transmissivity map (objective 1). Chapter 3 gives a detailed overview on datasets, methods and results for the intercomparison of the SCA products and the validation with high-resolution satellite images (objectives 2 and 3). The main findings are summarized in Chapter 4.

2 Development work during the VS-program and SCA datasets to be analysed

2.1 Introduction

The official SCA product SN-obs3 is based on the use of SCAmod-method by Metsämäki et al. (2005; 2012). The essential part of the SCAmod is the forest transmissivity map which was generated at SYKE and delivered to the Finnish Meteorological Institute (see Section 2.2 for more details). During the work within the Visiting Scientist (VS) program, it was found that the implementation of SCAmod, as to the use of the provided transmissivity data, was not quite correct. This led to a systematic overestimation of SCA compared to what would have been gained by a proper use of the transmissivity. This product is denoted as $\boldsymbol{SCA_{orig}}$ in this report. In addition, the product did not utilize the snow-free ground detection rule relaying on the NDVI-thresholding (Normalized Difference Vegetation Index); one purpose of the VS-work was to update the thresholding technique to the current state-of-the-art in order to take it into use in the SCA production.

The development work achieved within VS-program includes several points:

i) New transmissivity map, correctly used in the FMI processing software

ii) update of the NDVI-thresholding for detection of snow-free land ; inclusion of the thresholding in the operational production line

iii) Accounting for the neighbourhood of the product pixel: the current operational product has also neighbouring pixels contributing to the product values. First SCA is calculated for those pixels and then an average of the SCA's is assigned to product pixel. During the VS-work,

this procedure was changed so that first average reflectance is calculated from contributing pixels, and then SCAmod is applied to that reflectance value to retrieve the SCA.

As a result from these modifications, a candidate for the new operational SCA product is gained. In this report, this product is denoted as $\boldsymbol{SCA_{new}}$.

Due to the incorrect implementation as to the use of the transmissivity map, it was necessary to generate the dataset using the otherwise same SCA provision procedure as for $\boldsymbol{SCA_{orig}}$, but this time handling the transmissivity in a correct way. This is justified because if not done, the developments gained in within the VS-program would not be reflected in the resulting new product. Namely, basically it is expected that the update of transmissivity would increase the SCA particularly in forests, but when comparing $\boldsymbol{SCA_{new}}$ vs. $\boldsymbol{SCA_{orig}}$, this is not shown due to the overestimations occurring in $\boldsymbol{SCA_{orig}}$. The correctly implemented version of the product is denoted as $\boldsymbol{SCA_{orig\&correct}}$. Hence, $\boldsymbol{SCA_{new}}$ is compared with $\boldsymbol{SCA_{orig}}$ first, and then with $\boldsymbol{SCA_{orig\&correct}}$. The latter comparison would highlight the improvements made within the VS-work.

2.2 Updating the transmissivity map

2.2.1 Data and methods

The transmissivity map describes the transparency of a pixel, associated with the forest coverage and forest density, so that low transmissivitiy is associated with forests while non-forested areas are of high transmissivity. The transmissivity is a unitless measure, varying from 0 to 1, or alternatively from 0% to 100%. It can be derived using the SCAmod formula (Metsämäki et al., 2005) applied to reflectance acquisitions at the time of full snow cover. Since these observations are required for transmissivity calculations with SCAmod, it is necessary to obtain transmissivity estimates for pixels for which such observations are not available. Mostly this concerns areas in H-SAF geographical domain where seasonal snow cover is typically not observed. Metsämäki et al. (2012) introduced a method where local transmissivities are generated using combined information on SCAmod-based transmissivities (using reflectance acquisitions) and landcover data. In this approach, the land-cover classes are associated with a typical (average) transmissivity value based on statistical analysis between these two data sources. The applied landcover data is ESA GlobCover (Bicheron et al., 2008), and the SCAmod-based transmissivities were derived using Terra/MODIS top-of-atmosphere reflectance data from years 2005-2011. The methodology is described as follows:

In order to relate the GlobCover (GC) classes and their representative transmissivity, the class-stratified mean and standard deviation of transmissivity was determined using the already existing MODIS reflectance-derived transmissivity data over Europe. In the analysis, the transmissivity data had a resolution of 0.01°×0.01°, while GlobCover data was processed into a resolution of 0.0025°×0.0025°. These two were co-registered so that each transmissivity pixel matches with 4x4 GlobCover pixels. Whenever a clear majority of pixels represented one specific class, the transmissivity value contributed to the calculation of the class-wise transmissivity statistics (mean and standard deviation). After this was finalized, the transmissivity for each 0.01°×0.01° pixel of the whole target area can be expressed as a linear combination of class-wise average transmissivity and the class-wise occurrence of GlobCover pixels (4×4) falling into that pixel, as follows:

$$transmissivity_{i,j} = \sum_{c=1}^{N_{classes}(i,j)} \frac{n_{c,i,j}}{n_{tot,i,j}} * mean(t_{MODIS}(c)), \quad (1)$$

where

- i,j are grid cell coordinates (cell size 0.01°×0.01°)
- $n_{c,i,j}$ is number of GlobCover pixels of class c in within a grid cell i,j
- $n_{tot,i,j}$ is total number of GlobCover (0.0025°×0.0025°) pixels within grid cell (=16)
- $mean(t_{MODIS}(c))$ is the mean transmissivity for class c
- $N_{classes}(i,j)$ is the number of GlobCover classes within cell i,j.

The method described above was already taken into use for H-SAF SN-obs3 calculations in 2012. Since 2012, however, the statistical method has been further developed at SYKE, implying that the average typical transmissivity values are more representative particularly in the H-SAF geographical domain. In order to gain this improvement, ESA Global Albedo product was applied to distinguish between dense and very dense forests, which formally belong to a same class in GlobCover. By using albedo data for the maximum snow cover season, an additional forest class representing very dense forests was generated and associated with a more representative transmissivity value. Most importantly, this would mean that the earlier underestimated SCA values in very dense forests are now mapped with a higher accuracy. In addition to this improvement, also the MODIS-derived transmissivity underwent some changes, mostly related to a better selection of reflectance observations applied in the transmissivity calculation. This resulted in increased transmissivity values – again more representative - for some non-forested areas.

As a result, a new version of the transmissivity map was generated and delivered to FMI for production of a new set of SN-obs3 snow maps. This version was named v14.

2.2.2 Results

As stated above, the new transmissivity v14 is decreased for densely forested areas when compared to the earlier version applied in H-saf SN-obs3 production, while there is also an increase in higher transmissivities. All in all, the new transmissivity map introduces higher dynamics than the previous version. The histograms for both old and new transmissivity is presented in Figure 2.1~~Figure 2.1~~.

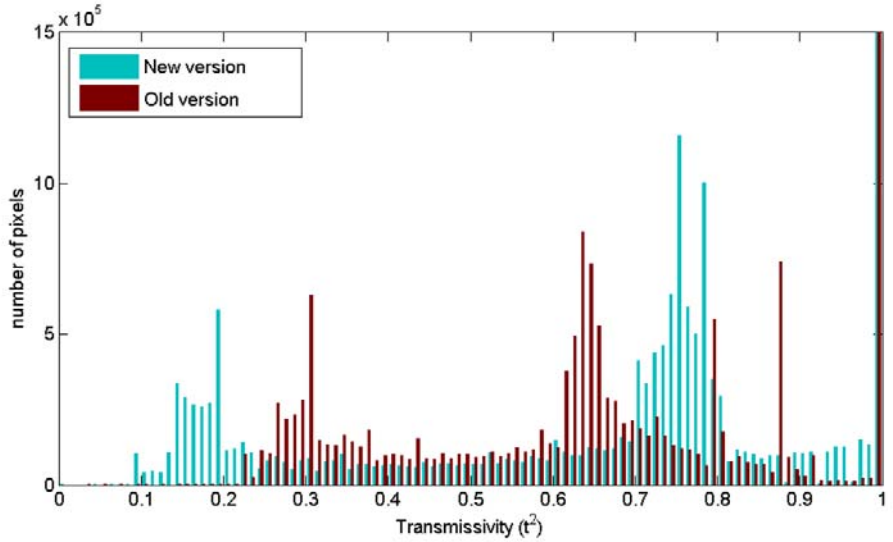

Figure 2.1. Histograms of the old and the new transmissivity maps for H-SAF SN-obs3 geographical domain.

The spatial map on the differences of the old and new transmissivity maps is presented in **Errore. L'origine riferimento non è stata trovata.**Figure 2.2~~Figure 2.2~~. The area with decreased value are clearly seen as yellowish colour in forested regions of Europe, while bluish colours highlights the increased transmissivity for some of the non-forested regions.

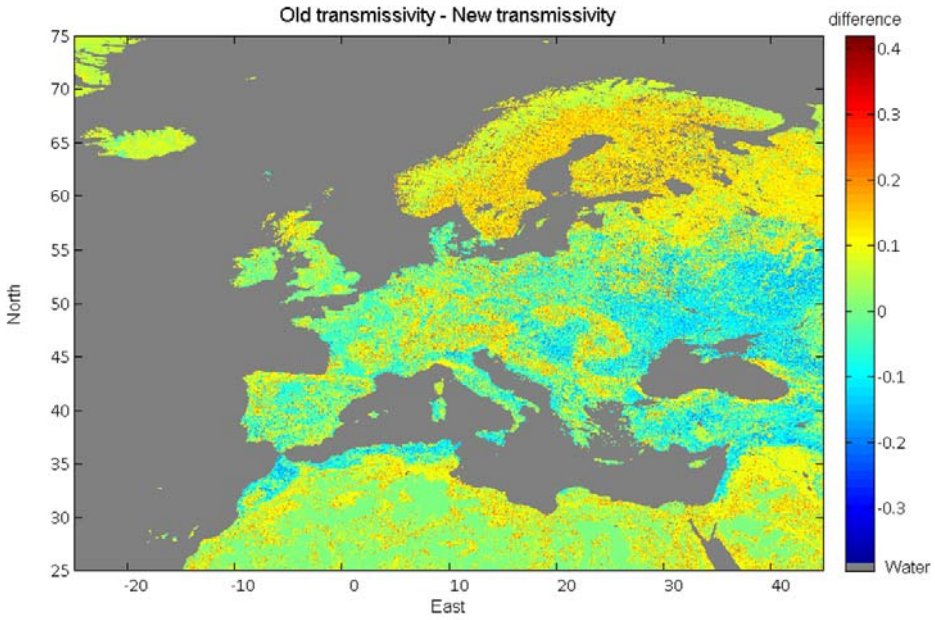

Figure 2.2. Difference between transmissivity maps (old version – new version). The total range of transmissivity is 0-1.

2.3 Rules for detection of snow-free ground

The SCAmod method is sensitive to the AVHRR band 1 (0.58-0.68 µm) reflectance so that the higher the reflectance, the higher is the resulting SCA. Although the SCAmod model includes a generally representative value for snow-free ground reflectance, the reflectance in reality may diverge from the applied value; if the real reflectance is higher than the applied one, SCA may be overestimated. To mitigate this problem, an additional decision technique based on NDSI (Normalized Difference Snow Index) and NDVI has been developed. From these two, NDSI is perhaps more efficient, but the necessary 1.6 µm bands is missing from AVHRR data (except for NOAA-17). Therefore the detection of snow-free land mostly relies on the NDVI. Earlier, a constant value was proposed for thresholding. During the VS-work, the thresholding procedure was changed in the way that the threshold depends on the local transmissivity value. This was deduced from an analysis made for confident snow-free pixels (verified with in-situ observations) and the corresponding NDVI and transmissivity. The new rule is:

$$\begin{aligned} &\text{NDVI\_threshold} = 0.142, \text{ when transsmissivity}^2 \in [0.7 - 1] \\ &\text{NDVI\_threshold} = -0.54 * \text{transmissivity}^2 + 0.52, \text{ when transsmissivity}^2 \in [0 - 0.7] \\ &\textbf{IF NDVI} \geq \textbf{NDVI\_threshold THEN SCA = 0\%.} \end{aligned} \quad (2)$$

In addition to the NDVI-thresholding, thresholding based on AVHRR Band 4 surface brightness temperature (BT11, 10.8µm) is also an effective way to screen the most confident snow-free areas. In the operational SCA-production, the temperature threshold was set to 288K. Since during the VS-work it was found that this high value leaves some false snow commissions particularly at mid-latitude, the threshold was decreased to 283K. The temperature thresholding rule is:

IF BT11 > 283K THEN SCA=0%. (3)

3 Intercomparison and validation against high resolution images

3.1 Data sets

3.1.1 H-SAF SCA product

The baseline dataset was processed using the operational algorithm used for the HSAF SCA product (H12) for flat and forested areas. AVHRR/3 data from NOAA-18 and NOAA-19 were used. The data were calibrated to top-of-atmosphere (TOA) reflectances using the coefficients provided by NOAA. The data set for this study covers the period from February to May 2014.

The resulting snow fractions were saved to HDF5 files (value range 0-100), and areas with clouds (value: 101), water (102), low solar angles (104) or no data (105) were masked accordingly. For ease of comparison, all data were projected to the nominal HSAF area of 25° to 75° North latitude and 25 ° West to 45° East longitude. Sampling for the grid is 0.01 degrees (resolution of approximately 2 km). In addition to the daily composites, also individual overpasses were saved.

During the VS-work, the processing software was adapted to use the updated transmissivity, which has a higher bit-depth than the original data. Furthermore, the way the satellite data are handled was changed. Instead of calculating the SCA values for each satellite pixel and averaging these values, an average TOA reflectance is first calculated for the target pixel and the SCA estimate is calculated from this value. These modifications were implemented into the processing system at FMI, in co-operation (as to the scientific considerations) with SYKE.

As already discussed in Section 2.1, three datasets were processed for the VS-study:

1) operational products, $\boldsymbol{SCA_{orig}}$. This version is hampered by the incorrect software implementation, leading to overestimated SCA;
2) re-processed operational products, $\boldsymbol{SCA_{orig\&correct}}$. Otherwise the same as above, but transmissivity correctly treated in the calculations;
3) A new product, including the enhancements developed within VS-program, $\boldsymbol{SCA_{new}}$.

3.1.2 Landsat 8 snow products for reference

Hemispherical-scale snow maps can be evaluated by comparing them to snow information derived from high-resolution imagery, with the assumption that these provide an appropriate approximation of the 'truth'. This is in practice the only option as there are only very limited *in situ* data, particularly on fractional snow cover, available. Landsat-8 OLI (Operational Land Imager) and TIRS (Thermal Infrared Sensor) data (year 2014) were employed to produce snow maps first in their nominal resolution (~ 0.00025°) which are then aggregated into the H12 resolution (0.01°).

The Landsat-8 scenes for spring period 2004 were selected and downloaded using the USGS (U.S. Geological Survey) interactive system. Several clear-sky scenes representing different stages of melting (SCA between 0-100%) were selected for the days when H12-product were available for the scene area. Nine scenes we chosen (see Figure 3.1~~Figure 3.1~~). A more detail description of the scenes are provided in Table 3.1.Landsat-8 scenes employed in the analyses.Table 3.1~~Table 3.1~~.

Table 3.1.Landsat-8 scenes employed in the analyses.

Scene number	Path(Row	Date	
1	175/24	08.03.2014	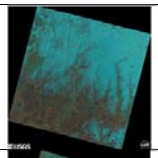
2	177/23	22.03.2014	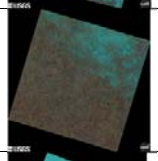
3	182/13	10.04.2014	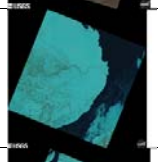
4	191/11	09.04.2014	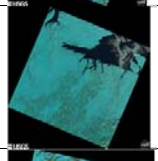
5	192/28	31.03.2014	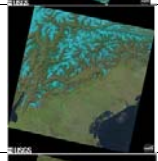
6	194/27	13.03.2014	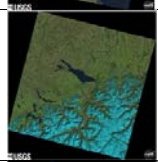
7	198/12	28.05.2014	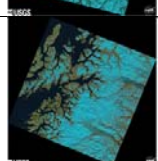
8	198/15	28.05.2014	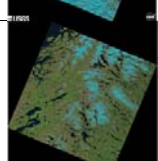
9	198/18	28.05.2014	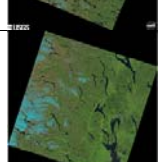

Pre-processing

The downloaded level 1b-data data were transformed into WGS-84 latitude/longitude grid with a resolution of 0.0025° × 0.0025° resolution using the software GDAL (http://www.gdal.org/;release-1600-

Codice campo modificato

gdal-1-10-mapserver-6-4). L8 OLI-bands 3 (0.544-0.590 µm), 4 (0.636-0.673 µm), 5 (0.851-0.879 µm) and 6 (1.566-1.651 µm) were processed as well as TIRS band 10 (10.60-11.19 µm).

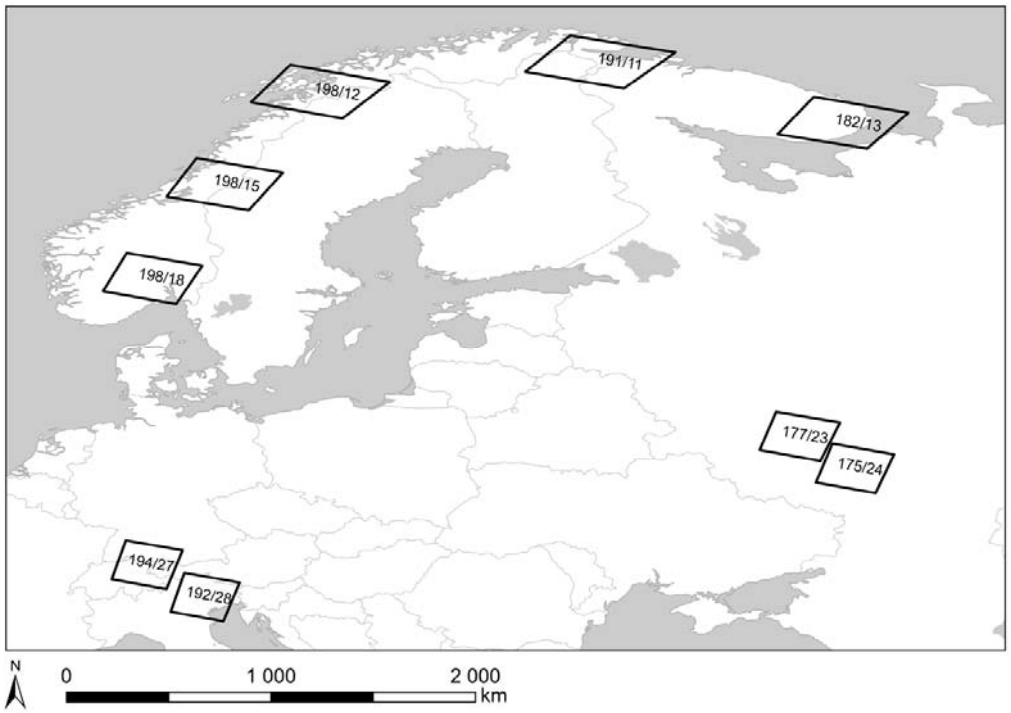

Figure 3.1. Landsat scenes used in validation of the HSAF SCA products.

Snow classification algorithm

Landsat-8 based snow maps were generated following the method by i) Salomonson and Appel (2006) and ii) Klein et al. (1998). These two methods were slightly modified as described in Metsämäki et al. (2015), the major modification being the use of temperature thresholding in the identification of snow-free areas. These methods provide snow information for high-resolution pixels, and the information can be aggregated into the coarse resolution grid to simulate the SCA estimates under evaluation, i.e. H12 in the 0.01° grid. Although the method by Salomonson and Appel (2006) as based on NDSI regression technique has a weaker performance for dense forest than for open or sparsely forested regions, (since it is designed to map the viewable snow instead of under-canopy snow) (Salomonson and Appel, 2004; Metsämäki et al., 2012; Niemi et al., 2012) it was decided here to use this approach uniformly for all TM/ETM+ scenes due to easy implementation of the methodology and also due to unavailability of better methods so far. However, the presence of forest must be taken into consideration when interpreting the results.

The binary snow mapping method by Klein et al. (1998) is based on NDSI-thresholding, with additional rules utilizing the NDVI as well as some reflectance thresholds. Basically this means that the method detects undercanopy snow ('snow on the ground'), correspondingly to SCAmod. This method classifies a pixel as 'snow' if its snow fraction is > ~50%, this percentage depending on the land cover. After binary mapping in L8 OLI 0.00025° resolution, the coarser resolution SCA can be retrieved by averaging the binary data. Although this technique may result in biased SCA, providing underestimations at low snow fractions and overestimations at high snow fractions (Rittger et al., 2013), these data are usable in evaluation of the performance of coarser resolution snow maps. It has also been found to identify snow in forests better than the Salomonson and Appel method (Salomonson and Appel, 2004; Rittger et al., 2013).

Overall, the processing steps starting from top-of atmosphere data include calculation of NDSI and NDVI, as well as brightness temperature for band 10. Band 10 is applied to identify warm surfaces so that whenever the temperature exceeds 288 K, the pixel is assigned as 'snow-free' (this is an addition to the Salomonson and Appel method and to the Klein method). Manually masked clouds and water pixels (according to the GlobCover classification) were excluded in the analysis. In this report the resulting Landsat8-based SCAmaps in the H12 resolution are denoted as $\boldsymbol{SCA_{klein}}$ and $\boldsymbol{SCA_{salapp}}$.

3.1.3 Ancillary data

The forest mask was derived from the ESA GlobCover land cover map (V2.2, Bicheron et al. 2009), reprojected to pixel size of 0.0025° (originally 300 m). The data consists of 64 classes, including several forest classes. For the forest mask in this study, 8 of them were selected. These were:

Table 3.2. ***The GlobCover classes used for the forest mask.***

50	*Closed (>40%) broadleaved deciduous forest (>5m)*
60	*Open (15-40%) broadleaved deciduous forest/woodland (>5m)*
70	*Closed (>40%) needleleaved evergreen forest (>5m)*
90	*Open (15-40%) needleleaved deciduous or evergreen forest (>5m)*
91	*Open (15-40%) needleleaved deciduous forest (>5m)*
92	*Open (15-40%) needleleaved evergreen forest (>5m)*
100	*Closed to open (>15%) mixed broadleaved and needleleaved forest (>5m)*
101	*Closed (>40%) mixed broadleaved and needleleaved forest (>5m)*

4 ×4 GlobCover pixels fall into the pixelsize of H12 SCA-product (0.01° resolution). In the generation of the 0.01° forest mask, a pixel was classified as 'forest' if 75% of the GlobCover pixels represent any of the forest classes described above.

3.2 Methods

3.2.1 Intercomparison of daily H12 SCA products

The comparison between the present H12 SCA products and the improved new H12 SCA products was carried out to see the effect of the developments made for the SCA retrieval within the VS-program. The comparison was accomplished in two steps described below. Because of the problem of the incorrect implementation in the production of $\boldsymbol{SCA_{orig}}$, we did not find it reasonable to compile a thorough comparison between $\boldsymbol{SCA_{new}}$ and $\boldsymbol{SCA_{orig}}$, as this would not reflect the advances gained by the updated transmissivity and the additional decision rules. Hence, only the first step of the analysis was performed between these two, whereas both steps were compiled for $\boldsymbol{SCA_{orig\&correct}}$ and $\boldsymbol{SCA_{new}}$.

1. Regression analysis of snow cover from the same day during the winter period and during snow melt:
   The following measures of comparison were used:

   R^2, the coefficient of determination (from Pearson r) between $\boldsymbol{SCA_{new}}$ and $\boldsymbol{SCA_{reference}}$, (4)

   $RMSD = \sqrt{\frac{1}{N}\sum\left(SCA_{new} - SCA_{reference}\right)^2}$, the Root Mean Square Deviation (5)

   $Bias = \frac{1}{N}\sum\left(SCA_{new} - SCA_{reference}\right)$. (6)

   $\boldsymbol{SCA_{reference}}$ refers to $\boldsymbol{SCA_{orig}}$ and $\boldsymbol{SCA_{orig\&correct}}$.

2. The amount of SCA differences ($\boldsymbol{SCA_{orig\&correct}}$ - $\boldsymbol{SCA_{new}}$) in daily products was determined from February to May 2014 and the mean difference for the whole period was calculated.

Pixels that were classified as "clear-sky" in both daily products were used in the comparison. The regression analysis was carried out for the whole H-SAF area (section 3.1.1) and all land cover classes. Additionally, the analysis was performed for forested and non-forested pixels using the forest mask described in section 3.1.3.

3.2.2 Metrics for validation with Landsat

The comparison between H12 SCA and Landsat-8 SCA is made as pixel-to-pixel analysis, which provided the statistical measures such as Bias and RMSD, as follows:

$$RMSD = \sqrt{\frac{1}{N}\sum\left(SCA_{H12} - SCA_{L8-reference}\right)^2} \quad (7)$$

$$Bias = \frac{1}{N}\sum\left(SCA_{H12} - SCA_{reference}\right) \quad (8)$$

3.3 Results

3.3.1 Intercomparison of daily H12 SCA products

The results for the overall comparison of daily SCA products from February to May 2014 are shown in Figure 3.2~~Figure 3.2~~. Overall, a good agreement was found between $\boldsymbol{SCA_{new}}$ and the two product versions $\boldsymbol{SCA_{orig}}$ and $\boldsymbol{SCA_{orig\&correct}}$ (Figure 3.2~~Figure 3.2~~). As expected, we observed a negative bias between $\boldsymbol{SCA_{orig}}$ and $\boldsymbol{SCA_{new}}$, which originates from the systematic overestimations in $\boldsymbol{SCA_{orig}}$ due to the incorrect implementation. In contrast to that, the bias was positive for the comparison with $\boldsymbol{SCA_{orig\&correct}}$, showing the effect of the adaptation of the new transmissivity v14. This increase is more distinctive in case of forests (Figure 3.3~~Figure 3.3~~ a) where the transmissivity values underwent the biggest change (Figure 2.2~~Figure 2.2~~). This is also highlighted in the spatial map on the mean differences, made separately for all pixels and forested pixels (Figure 3.3~~Fig 3.4~~). SCA for forested pixels, based on the application of the transmissivity map v14 and the implementation of the other changes described in section 2, was in mean 9% higher than for $\boldsymbol{SCA_{orig\&correct}}$ **(**Figure 3.3~~Figure 3.3~~ ***a)***. The largest increase of SCA takes place in forested areas in central Finland and Sweden, Russia and in the Alps.

As expected, the increase of SCA in dense forest cannot be depicted from the comparison of $\boldsymbol{SCA_{new}}$ with $\boldsymbol{SCA_{orig}}$, because the incorrect implementation of transmissivity in this version resulted in an overestimation of SCA. Therefore, $\boldsymbol{SCA_{new}}$ decreased slightly for both forested and non-forested pixels in comparison to $\boldsymbol{SCA_{orig}}$ (Figure 3.5).

The correspondence between the $\boldsymbol{SCA_{new}}$ and $\boldsymbol{SCA_{orig\&correct}}$ was very high for non-forested pixels, which showed in average a small increase in SCA of 0.8% (Figure 3.3~~Figure 3.3~~ b). From Figure 3.4~~Figure 3.4~~, a mean decrease of SCA was observed in south-western Russia and in parts of Turkey, Georgia and Azerbaijan. These are non-forested areas with seasonal snow cover where the transmissivity increased in v14.

The bias and RMSD between $\boldsymbol{SCA_{new}}$ and $\boldsymbol{SCA_{orig\&correct}}$ in forested areas varied for individual daily composites and showed a decreasing trend from end of February towards the end of snow melt (Figure 3.6~~Figure 3.6~~). Bias and RMSD ranged between 0.41 and 12.74% and 2.74 and 20.74 %, respectively.

(a)

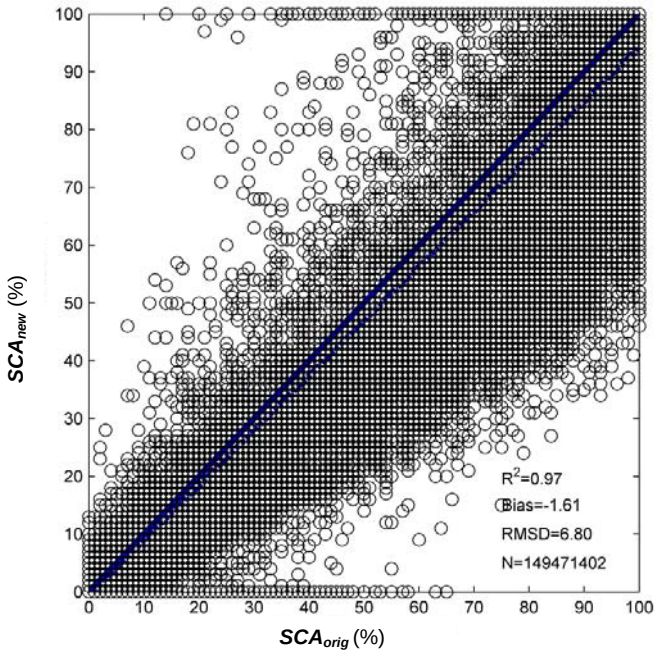

(b)

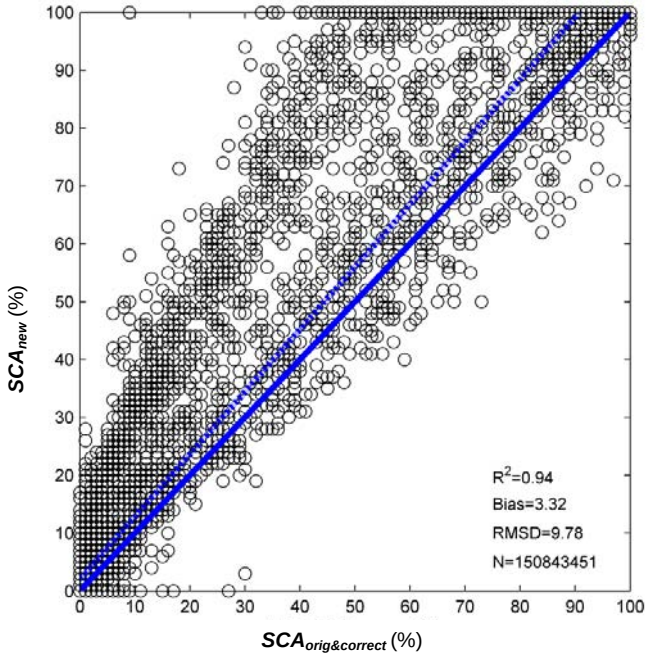

Figure 3.2. Comparison of H12 SCA daily product: (a) SCA_{orig} to SCA_{new} (b) $SCA_{orig\&correct}$ to SCA_{new}. The blue line gives the 1:1 line and the broken blue line indicates the linear regression line between reference data and SCA_{new}. Only every 1.000th (a) and 10.000th (b) comparison pair is shown in the figure.

(a)

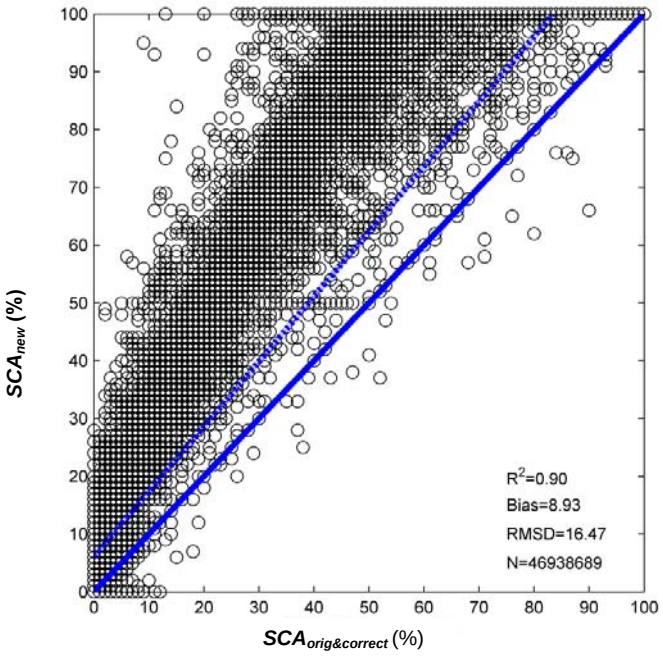

(b)

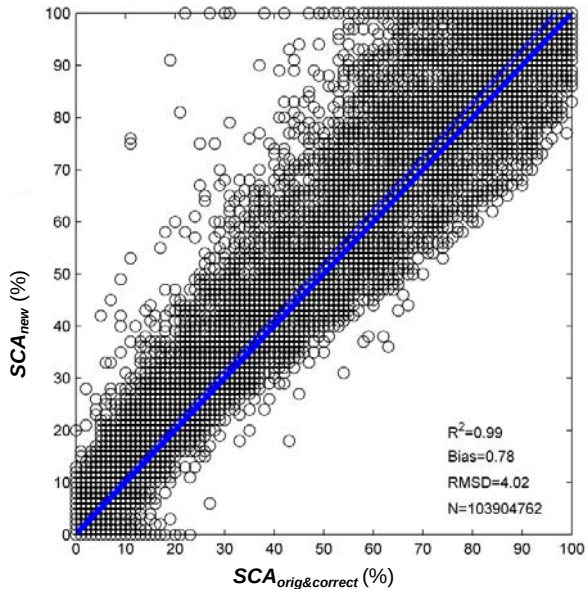

Figure 3.3. Comparison between H12 SCA daily product based on new transmissivity (SCA_{new}) with $SCA_{orig\&correct}$): (a) for forested pixels and (b) for non-forested pixels. The blue line gives the 1:1 line and the broken blue line indicates the linear regression line between $SCA_{orig\&correct}$ and SCA_{new}. Only every 1.000th comparison pair is shown in the figures.

(a)

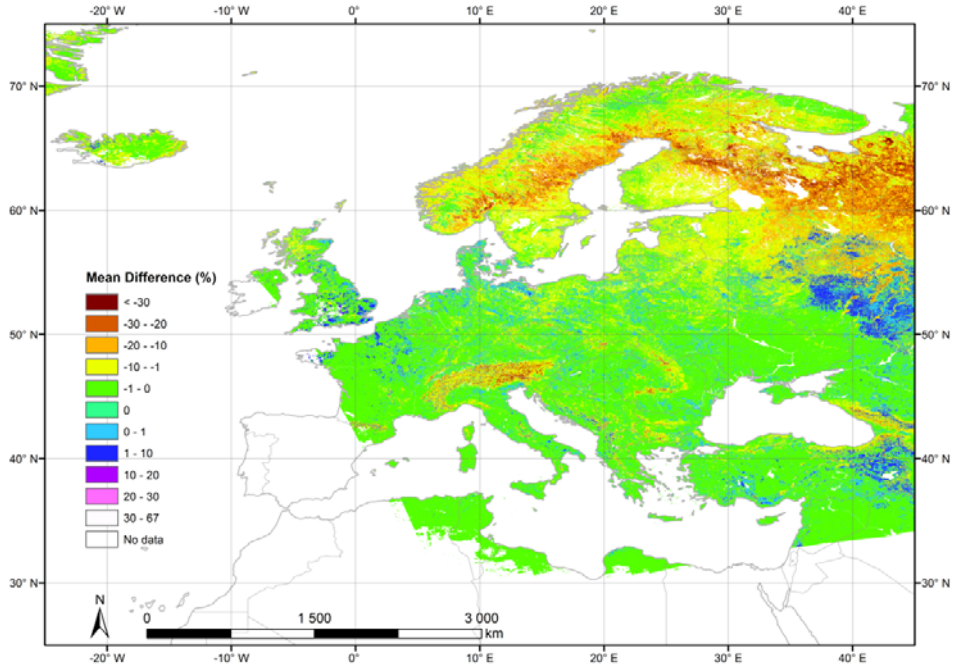

(b)

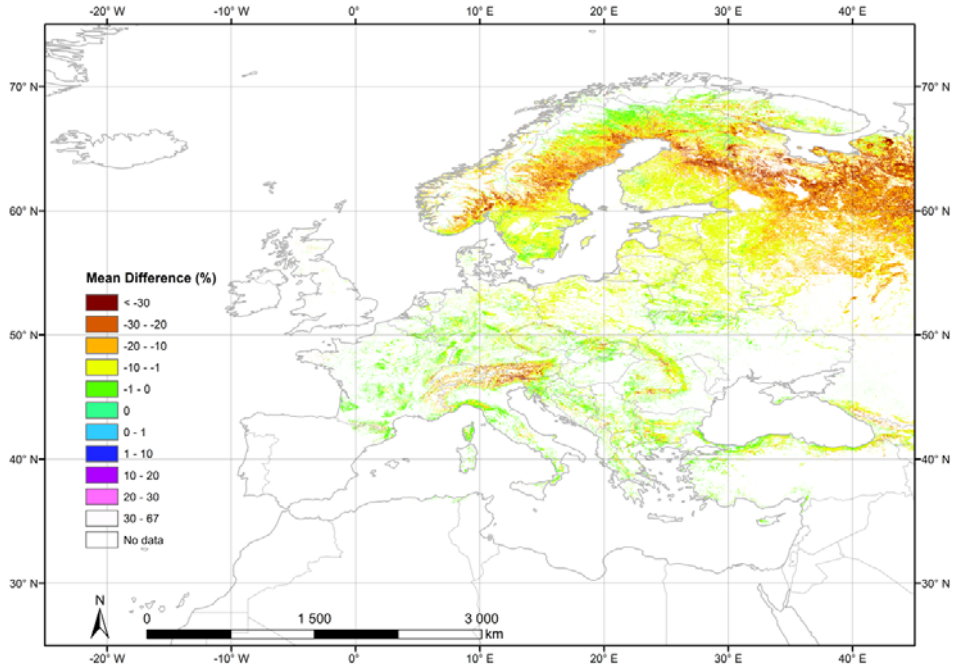

Figure 3.4. Mean difference ($SCA_{orig\&correct} - SCA_{new}$) between H12 SCA daily products for the period from February to May 2014: (a) for all pixels and (b) for pixels with forest cover.

(a)

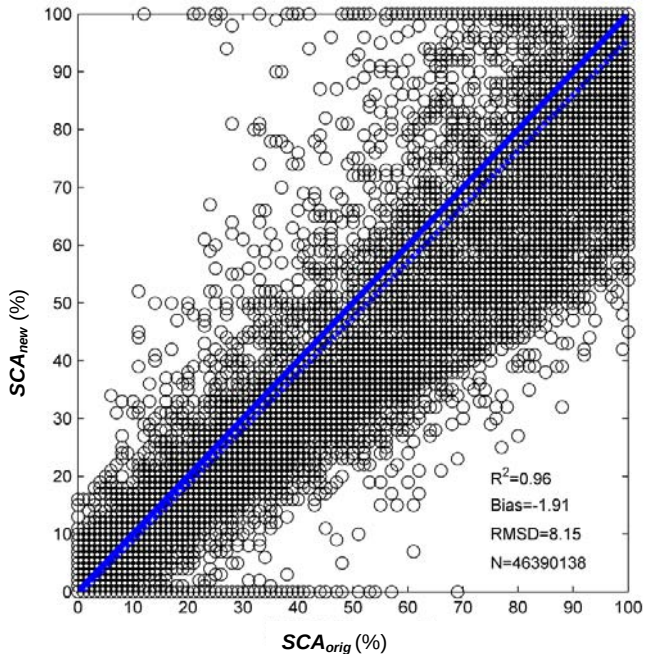

(b)

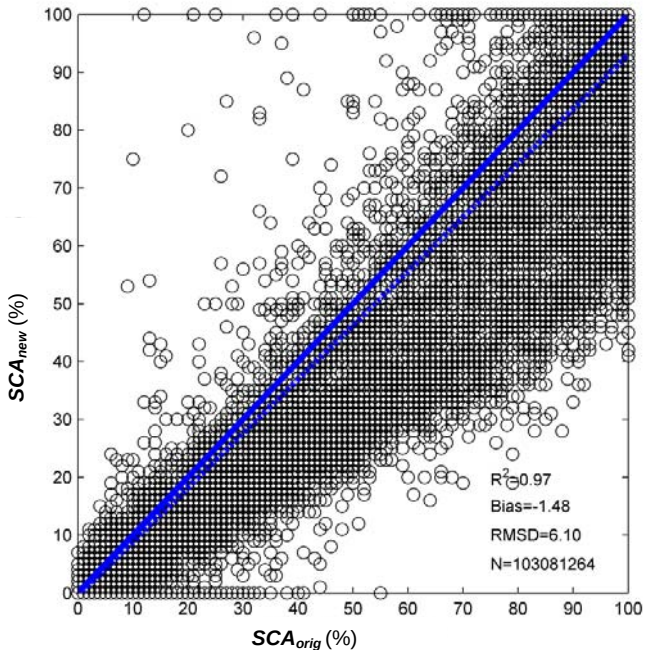

Figure 3.5. Comparison between H12 SCA daily product based on new transmissivity (SCA_{new}) with SCA_{orig}): (a) for forested pixels and (b) for non-forested pixels. The blue line gives the 1:1 line and the broken blue line indicates the linear regression line between SCA_{orig} and SCA_{new}. Only every 1.000th comparison pair is shown in the figures.

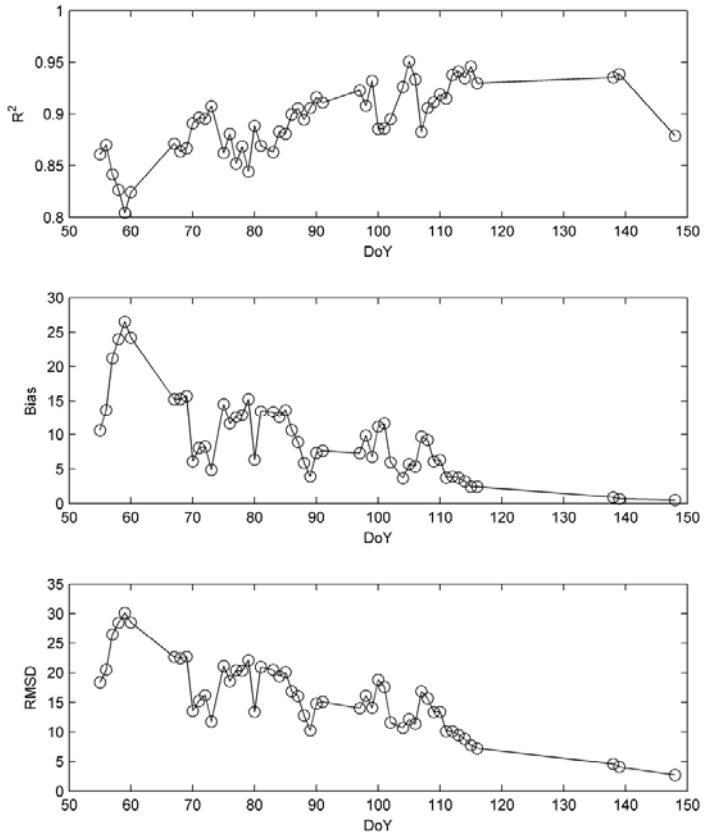

Figure 3.6. Time series of R^2, Bias and RMSD for the comparison of daily SCA_{new} with $SCA_{orig\&correct}$ for pixels with forest cover in 2014. DoY, day of year.

3.3.2 Validation against Landsat-8 high-resolution images

The snow conditions within Landsat-8 scenes vary from very limited snow to almost full snow cover, as shown in Figure 3.7. This ensures that the whole range of SCA is covered in the analysis. The RMSD and Bias for each L8-scene are presented in Figure 3.8. The analyses were made separately for the reference data represented by SCA_{klein} and SCA_{salapp} It is worth noting that the results are severely hampered by the poor geolocation of the H12 SCA products. This causes that we are actually comparing maps that are not correctly co-registered into the same grid (i.e. there is a 1-2 km shift between the product and the reference data. This has a significant deteriorating effect on the validation result; the effect being the stronger the more fragmented the landscape and the snow layer is.

For the analysed 9 scenes, RMSD varies from ~7%-units to 28 %-units; bias varies from -14 %-units to 6 %-units, see Fig 3.8. The average RMSD calculated from all scenes is 19.2 %-units using SCA_{klein}, and 18.8 %-units when using SCA_{salapp} Lansat-8-derived references. The average Bias using SCA_{klein} is -2.9 while the Bias with SCA_{salapp} is -2.2. The average Bias is strongly dominated by scene #2., which provides a clearly larger negative bias than the other ones. The reason for this distinctive value remains

unclear: the scene has low snow fraction in general (see Figure 3.7) which H12 SCA cannot recognize properly.

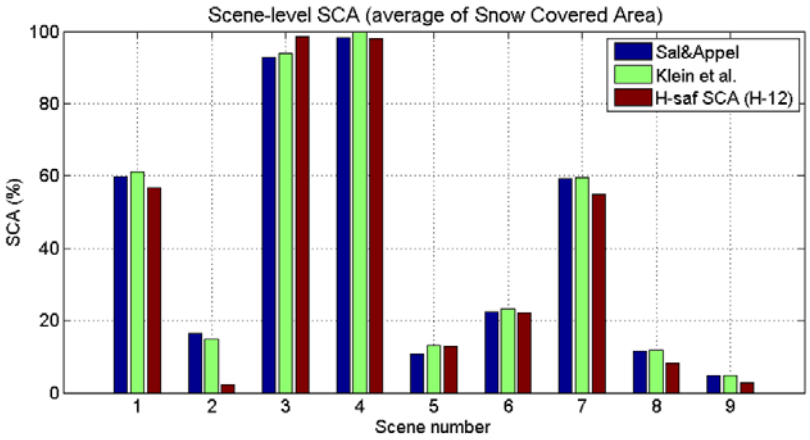

Figure 3.7. The average value of Fraction of Snow Covered area (SCA_{new}) for the Landsat-8 scenes.

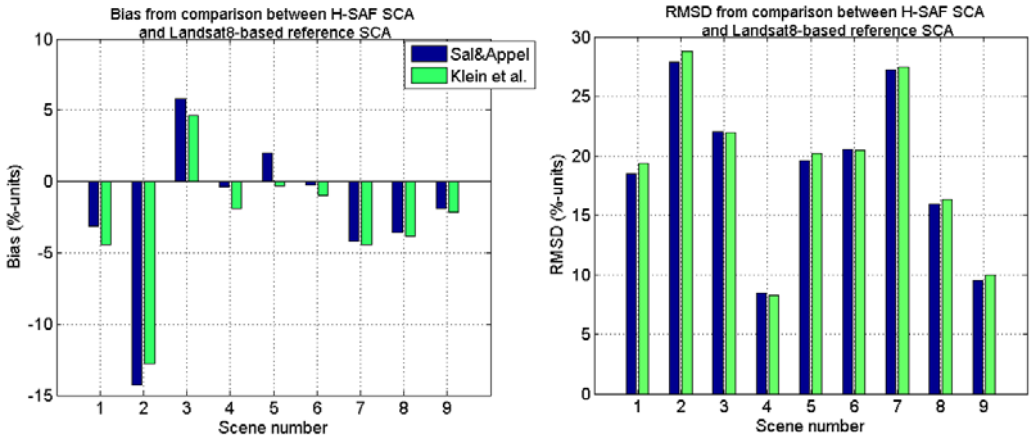

Figure 3.8. The result from comparison between Landsat-8 reference SCA and H12 SCA_{new}. *Left*: **Bias;** *Right*: **RMSD.**

An example of the analysed data for scene #9, Southern Norway, is provided in Figure 3.9. The two snow maps in the upper pane show the snow maps (H12 SCA on the left, SCA_{salapp} on the right. The lower pane shows the scatterplots for H12 SCA vs. SCA_{klein} and H12 SCA vs. SCA_{salapp}. From the scatterplots one can see that for this scene the pixel-to-pixel comparison shows a good performance for the H12 SCA; indeed, RMSD for this scene is 9.98 (SCA_{klein}) and 9.48 (SCA_{salapp}).

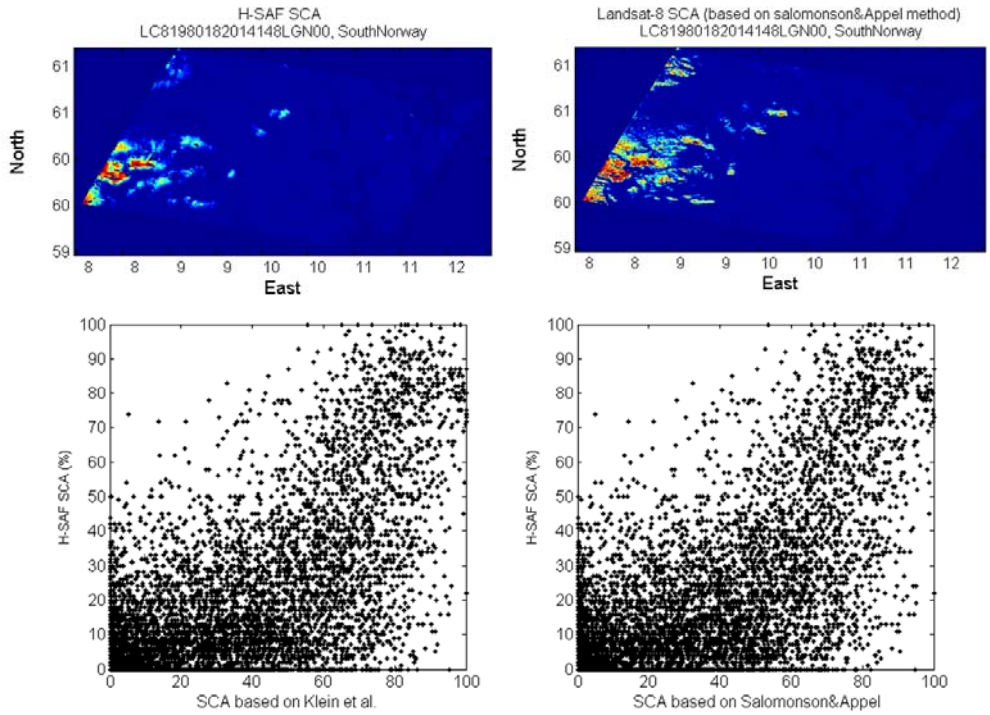

Figure 3.9. $SCA_{reference}$ (derived from Landsat-8) and SCA_{new} for scene #9, LC81980182014148LGN00, South Norway, 28.5.2014. *TopLeft*: **SCA_{new}**, *TopRight*: **SCA_{salapp}**, *BottomLeft*: **scatterplot on SCA_{klein} vs. SCA_{new}**, *Bottom Right*: **scatterplot on SCA_{salapp} vs. SCA_{new}.**

4 Summary and conclusion

The aim of the visiting scientist work was the improvement of the quality of H12 (formerly sn-obs3) SCA product. Since this goal is heavily dependent on the representativeness of the forest transmissivity used by the SCA-method (*SCAmod*), an emphasis was put on the update of the transmissivity. This was successfully accomplished. At the time of implementation of the updated transmissivity for the operational H12 processing line, it was found that the use of the transmissivity had been incorrect in the processing code. This has caused overestimation of SCA. The code was corrected as to the use of transmissivity and the products using the old transmissivity were re-processed. This was done in order to see the effect of the transmissivity update to the SCA-estimates. For the new SCA product, also other improvements were made, regarding the detection of snow-free pixels and the way the product pixel is generated from the original AVHRR data using the neighbouring pixels as well.

The difference between the current operational H12 SCA product and the new SCA product was investigated. The comparison of the SCA products was focused on the new improved SCA and the re-processed H12, as it was not reasonable to put much effort to the investigation of the version with the incorrect implementation. The results evidently show that the updated transmissivity increases the SCA particularly in forested areas, which was expected as the biggest changes in the updated transmissivity concerned the forests.

The validation using high-resolution Landsat8-data was performed for the new improved SCA. The results indicate an average RMSE of 19 %-units. This result was much affected by the poor geolocation

accuracy of H12 SCA (shift of 1-2 km compared to true location), which means that the pixel-by pixel comparison actually handled SCA maps not co-registered in the same grid. a better geolocation would most likely improve the validation results.
However, even the gained RMSD < 20% is typically the limit that is accepted by users.

5 References

Klein, A. G., Hall, D. K. & Riggs, G. A. (1998). Improving snow-cover mapping in forests through the use of a canopy reflectance model. *Hydrological Processes*, 12, 1723–1744.

Bicheron, P., Huc, M., Henry, C., & Bontemps, S. (2008). GLOBCOVER Product Description Manual, Issue 2, Rev. 2, 4/12/2008.

Metsämäki S.J., Anttila S.T., Markus H.J. & Vepsäläinen J.M. 2005. A feasible method for fractional snow cover mapping in boreal zone based on a reflectance model. *Remote Sensing of Environment* 95: 77-95.

Metsämäki, S., Mattila, O.-P., Pulliainen, J., Niemi, K., Luojus, K., Böttcher, K. (2012). An optical reflectance model-based method for fractional snow cover mapping applicable to continental scale. *Remote Sensing of Environment, 123, 508-521.*

Niemi, K., Metsämäki, S., Pulliainen, J., Suokanerva, H., Böttcher, K., Leppäranta, M., Pellikka, P. (2012). The behaviour of mast-borne spectra in a snow-covered boreal forest. *Remote Sensing of Environment,* 124, 551-563.

Rittger, K., Painter, T. H. & Dozier, J. (2013). Assessment of methods for mapping snow cover from MODIS. *Advances in Water Resources*, 51, 367–380.

Salomonson, V. V. & Appel, I. (2004). Estimating fractional snow cover from MODIS using the normalized difference snow index. *Remote Sensing of Environment*, 89, 351–360.

Salomonson, V. V. & Appel, I. (2006). Development of the Aqua MODIS NDSI fractional snow cover algorithm and validation results. *IEEE Transactions on Geoscience and Remote Sensing*, 44, 1747–1756.